Precise predictions for Higgs production in association with top quarks

Ansgar Denner, Würzburg

HEPKIT 2015, Karlsruhe, October 5–8, 2015

in collaboration with Robert Feger

published in JHEP 1504 (2015) 008 [arXiv:1412.5290] and arXiv:1506.07448

- Introduction
- Irreducible background and interference effects
- NLO QCD corrections to $\mathrm{pp} \to \mathrm{W^+W^-b\bar{b}H}$
- Conclusions

Introduction

Higgs boson observed $\Rightarrow$ investigate its properties $\Rightarrow$ measure its couplings

important process: associated Higgs production with top-antitop quarks:

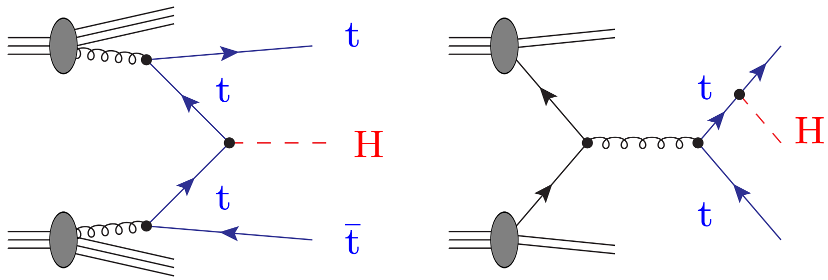

- allows direct measurement of top Yukawa coupling ($\mathrm{Ht\bar{t}}$ coupling)
- small cross section: $\sigma \approx 500\,\mathrm{fb}$ at $13\,\mathrm{TeV}$
- large background from $\mathrm{t\bar{t}b\bar{b}}$, $\mathrm{t\bar{t}jj}$ renders analysis extremely difficult
- need improved experimental analyses (like highly boosted Higgs bosons) and precise theoretical predictions for signal and background
- results from LHC run I:
  CMS '15: $\mu = 1.2 + 1.6 - 1.5$ for $\sigma(\mathrm{t\bar{t}H})$, $\mathrm{H} \to \mathrm{b\bar{b}}$
  ATLAS '15: $\mu = 1.5 \pm 1.1$ for $\sigma(\mathrm{t\bar{t}H})$, $\mathrm{H} \to \mathrm{b\bar{b}}$

Experimentally relevant processes

Production processes

- $\mathrm{pp} \to \mathrm{t\bar{t}H} \to \mathrm{W^+W^-b\bar{b}H} \to \mathrm{l}\nu_l \mathrm{jjb\bar{b}H}$
- $\mathrm{pp} \to \mathrm{t\bar{t}H} \to \mathrm{W^+W^-b\bar{b}H} \to \mathrm{l}\nu_l \mathrm{l'}\nu_l \mathrm{b\bar{b}H}$

decay processes

$\mathrm{H} \to \mathrm{b\bar{b}}, \tau^+\tau^-, \mathrm{ZZ}, \mathrm{WW}$

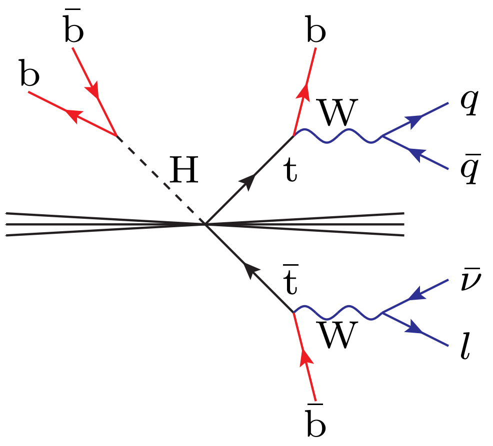

$\mathrm{pp} \to \mathrm{l}\nu_l \mathrm{jjb\bar{b}b\bar{b}}$

- complicated final state
- experimentally and theoretically challenging

this talk:

- study of irreducible background and interference effects for $\mathrm{pp} \to \mathrm{l}\nu_l \mathrm{jjb\bar{b}b\bar{b}}$
- results for NLO QCD corrections for $\mathrm{pp} \to \mathrm{e}^+\nu_\mathrm{e}\mu^-\bar{\nu}_\mu \mathrm{b\bar{b}H}$

Irreducible background and interference effects

Process $\mathrm{pp} \to \mathrm{t\bar{t}H} \to \mathrm{l^+\nu_l jjb\bar{b}b\bar{b}}$

Three scenarios: scenario 1

- $\mathrm{t\bar{t}H}$ production: $\mathrm{pp} \to \mathrm{t\bar{t}H} \to \mathrm{l^+\nu_l jjb\bar{b}b\bar{b}}$
  - intermediate t, $\mathrm{\bar{t}}$, H required
    treated in pole approximation
  - gluon–gluon partonic channels $\mathrm{gg} \to \mathrm{l^+\nu_l}q'\bar{q}''\mathrm{b\bar{b}b\bar{b}}$
    order of amplitude: $\mathcal{O}(\alpha_s\alpha^3)$
    quark–antiquark partonic channels $q\bar{q} \to \mathrm{l^+\nu_l}q'\bar{q}''\mathrm{b\bar{b}b\bar{b}}$
    order of amplitude: $\mathcal{O}(\alpha_s\alpha^3)$, $\mathcal{O}(\alpha^4)$
  - sample diagrams

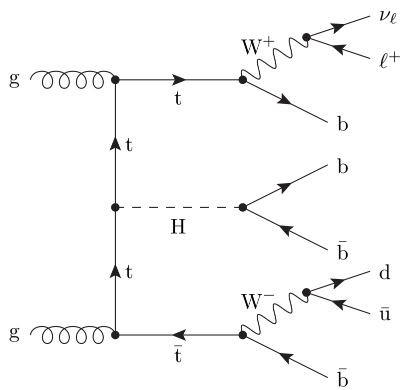

$\mathcal{O}(\alpha_s\alpha^3)$

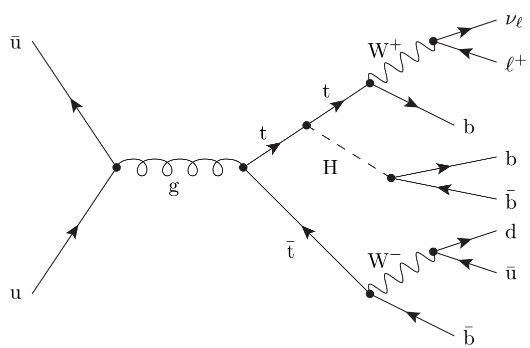

$\mathcal{O}(\alpha_s\alpha^3)$

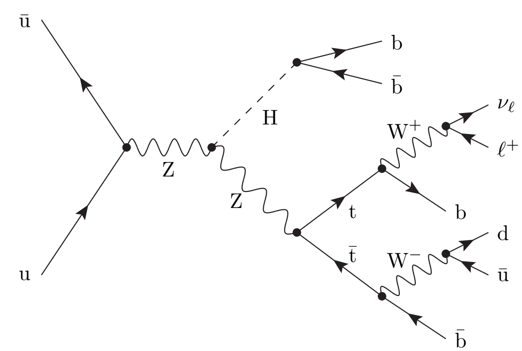

$\mathcal{O}(\alpha^4)$

Process $\mathrm{pp} \to \mathrm{t\bar{t}b\bar{b}} \to \mathrm{l^+\nu_l jjb\bar{b}b\bar{b}}$

Scenario 2

- $\mathrm{t\bar{t}b\bar{b}}$ production $\mathrm{pp} \to \mathrm{t\bar{t}b\bar{b}} \to \mathrm{l^+\nu_l jjb\bar{b}b\bar{b}}$
  - intermediate $\mathrm{t}, \bar{\mathrm{t}}$ required, treated in pole approximation
    no resonant Higgs required
  - same partonic channels as above
    additional $\mathcal{O}(\alpha_s^2\alpha^2)$ contributions for gg and $q\bar{q}'$ channels ($\mathrm{H} \to \mathrm{g}$)
    (plus contributions with $\mathrm{H} \to \mathrm{Z}, \gamma, \mathrm{W}$)
  - sample diagrams

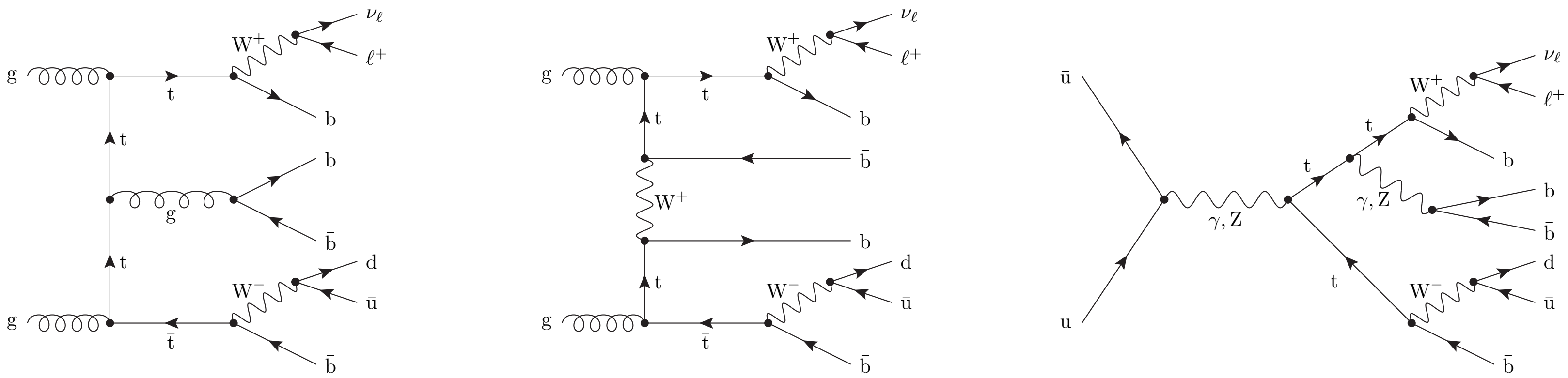

$\mathcal{O}(\alpha_s^2\alpha^2)$ $\mathcal{O}(\alpha_s\alpha^3)$ $\mathcal{O}(\alpha^4)$

Process $\mathrm{pp} \to \mathrm{l}^+\nu_\mathrm{l}\mathrm{jjb\bar{b}b\bar{b}}$

Scenario 3

- full process $\mathrm{pp} \to \mathrm{l}^+\nu_\mathrm{l}\mathrm{jjb\bar{b}b\bar{b}}$
  - complete set of diagrams: no resonances required
  - # of channels increases by more than factor 4 owing to crossing symmetric channels
  - amplitude receives contributions of $\mathcal{O}(\alpha^4)$, $\mathcal{O}(\alpha_\mathrm{s}\alpha^3)$, $\mathcal{O}(\alpha_\mathrm{s}^2\alpha^2)$ and $\mathcal{O}(\alpha_\mathrm{s}^3\alpha)$
    up to 78052 diagrams for individual channels! (unitary gauge)
  - sample diagrams

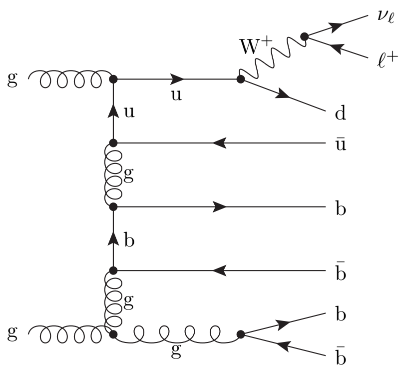

$\mathcal{O}(\alpha_\mathrm{s}^3\alpha)$

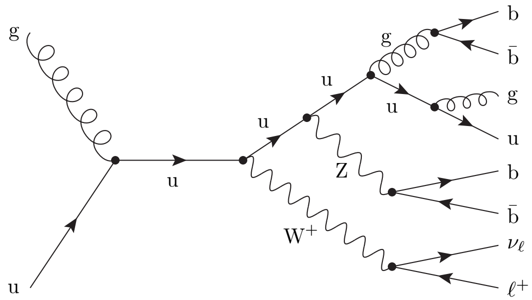

$\mathcal{O}(\alpha_\mathrm{s}^2\alpha^2)$

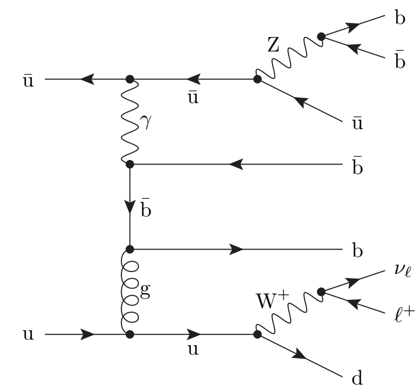

$\mathcal{O}(\alpha_\mathrm{s}\alpha^3)$

Calculational setup

- complex-mass scheme for unstable particles
  (not treated in pole approximation)

  Denner, Dittmaier, Roth, Wieders '99
- on-shell projection of momenta
  for resonances treated in pole approximation
  such that invariants of other resonances are not shifted!
- massless light quarks, massive b quarks
- only PDFs of light quarks included $(\mathrm{u}, \mathrm{d}, \mathrm{c}, \mathrm{s})$ besides gluons
- all matrix elements calculated with RECOLA (recursive algorithm)

  Actis et al.
- phase-space integration: multi-channel Monte Carlo
  $\Rightarrow$ number of diagrams matters

Setup for numerics

- collider energy: $13\,\mathrm{TeV}$
- scale choice: Beenakker et al. '03
  $\mu = \mu_\mathsf{R} = \mu_\mathsf{F} = \frac{1}{2}\,(2m_t + m_H) = 236\,\mathrm{GeV}$
- PDFs: CT10 Lai et al. '10
- input parameters:

$$m_\mathrm{t} = 173\,\mathrm{GeV}, \qquad \Gamma_\mathrm{t} = 1.47\,\mathrm{GeV}, \qquad m_\mathrm{b} = 4.8\,\mathrm{GeV}$$
$$M_\mathrm{H} = 126\,\mathrm{GeV}, \qquad M_\mathrm{Z}^\mathsf{OS} = 91.1876\,\mathrm{GeV}, \qquad M_\mathrm{W}^\mathsf{OS} = 80.385\,\mathrm{GeV}$$
$$\Gamma_\mathrm{H} = 4.21 \times 10^{-3}\,\mathrm{GeV}, \qquad \Gamma_\mathrm{Z}^\mathsf{OS} = 2.4952\,\mathrm{GeV}, \qquad \Gamma_\mathrm{W}^\mathsf{OS} = 2.0850\,\mathrm{GeV}$$

- cuts:

$$p_{\mathsf{T},\mathrm{j}} > 25\,\mathrm{GeV}, \qquad |y_\mathrm{j}| < 2.5, \qquad \Delta R_\mathrm{jj} > 0.4$$
$$p_{\mathsf{T},\mathrm{b}} > 25\,\mathrm{GeV}, \qquad |y_\mathrm{b}| < 2.5, \qquad \Delta R_\mathrm{bb} > 0.4 \qquad \Delta R_\mathrm{jb} > 0.4$$
$$p_{\mathsf{T},\mathrm{l}^+} > 20\,\mathrm{GeV}, \qquad |y_{\mathrm{l}^+}| < 2.5, \qquad p_{\mathsf{T},\mathsf{miss}} > 20\,\mathrm{GeV}$$

- b quarks originating from t and $\bar{\mathrm{t}}$ quark are selected according to

$$\mathcal{L} \propto \frac{1}{\left(p^2_{\mathrm{l}^+\nu_\mathrm{l}\mathrm{b}_i} - m_\mathrm{t}^2\right)^2 + (m_\mathrm{t}\Gamma_\mathrm{t})^2}\,\frac{1}{\left(p^2_{\mathrm{j}_1\mathrm{j}_2\mathrm{b}_j} - m_\mathrm{t}^2\right)^2 + (m_\mathrm{t}\Gamma_\mathrm{t})^2}$$

Cross section for $\mathrm{pp} \to \mathrm{t\bar{t}H} \to \mathrm{l^+\nu_l jjb\bar{b}b\bar{b}}$

$\mathrm{pp} \to \mathrm{t\bar{t}H} \to \mathrm{l^+\nu_l jjb\bar{b}b\bar{b}}$ (at leading order)

	cross section [fb]			
	$\mathcal{O}\left((\alpha^4)^2\right)$	$\mathcal{O}\left((\alpha_s\alpha^3)^2\right)$	total	fraction [%]
$q\bar{q}$	0.014887(2)	2.1467(2)	2.1621(2)	29
gg	–	5.230(1)	5.2298(9)	71
$\sum$	0.014887(2)	7.377(1)	7.3920(9)	100

- 70% from gg processes
- $\mathcal{O}\left((\alpha_s\alpha^3)^2\right)$ dominates
- pure EW contribution $\mathcal{O}\left((\alpha^4)^2\right)$ tiny
- no interferences between different orders
  owing to colour matrices

Cross section for $\mathrm{pp} \to \mathrm{t\bar{t}b\bar{b}} \to \mathrm{l^+\nu_l jjb\bar{b}b\bar{b}}$

$\mathrm{pp} \to \mathrm{t\bar{t}b\bar{b}} \to \mathrm{l^+\nu_l jjb\bar{b}b\bar{b}}$ (at leading order)

	cross section [fb]					
	$\mathcal{O}((\alpha^4)^2)$	$\mathcal{O}((\alpha_s\alpha^3)^2)$	$\mathcal{O}((\alpha_s^2\alpha^2)^2)$	sum	total	fraction [%]
$q\bar{q}$	0.018134(6)	2.4932(9)	0.9199(2)	3.4312(9)	3.4366(6)	13
gg	–	7.818(4)	16.650(9)	24.47(1)	23.010(7)	87
$\sum$	0.018134(6)	10.311(4)	17.570(9)	27.90(1)	26.446(7)	100

- Irred. background from $\mathrm{t\bar{t}b\bar{b}}$: $\sigma^{\text{Irred.}}_{\mathrm{t\bar{t}b\bar{b}}} = 19.06\,\mathrm{fb} = (26.45 - 7.39)\,\mathrm{fb}$ (260%)
  mainly from QCD production (Higgs replaced by gluon)
  additional background from Z bosons ($\mathrm{t\bar{t}Z}: 1.01\,\mathrm{fb}$), W bosons and photons

- Negative interferences between different orders:
  $< 0.2\%$ in $q\bar{q}$, 6% in gg, 5% for $\sigma_{\mathrm{t\bar{t}b\bar{b}}}$
  main source:
  interferences of dominant QCD diagrams with t-channel W-exchange diagrams
  signal–background interference $< 1\%$

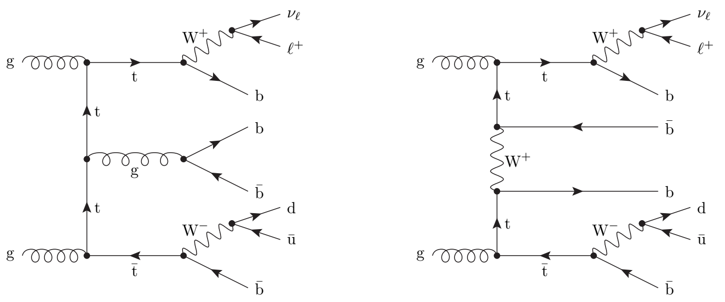

Cross section for $\mathrm{pp} \to \mathrm{l}^+\nu_\mathrm{l}\mathrm{jjb\bar{b}b\bar{b}}$

$\mathrm{pp} \to \mathrm{l}^+\nu_\mathrm{l}\mathrm{jjb\bar{b}b\bar{b}}$ (at leading order)

	cross section [fb]						
	$\mathcal{O}\big((\alpha^4)^2\big)$	$\mathcal{O}\big((\alpha_\mathrm{s}\alpha^3)^2\big)$	$\mathcal{O}\big((\alpha_\mathrm{s}^2\alpha^2)^2\big)$	$\mathcal{O}\big((\alpha_\mathrm{s}^3\alpha)^2\big)$	sum	total	fraction [%]
$\mathrm{g}q$	–	0.231(4)	0.370(2)	0.365(1)	0.966 (4)	0.944 (9)	3.3
$\mathrm{g}\bar{q}$	–	0.0421(6)	0.0679(3)	0.0608(2)	0.1708(7)	0.167 (1)	0.6
$qq^{(\prime)}$	0.001471(2)	0.0575(5)	0.1106(2)	0.07871(9)	0.2483(6)	0.2478(8)	0.9
$q\bar{q}$	0.01973(3)	2.531(6)	0.957(1)	0.00333(1)	3.511 (6)	3.538 (4)	12.4
gg	–	8.01(2)	17.19(6)	0.00756(2)	25.21 (6)	23.71 (6)	82.9
$\sum$	0.02120(3)	10.87(2)	18.69(6)	0.516(2)	30.10 (6)	28.60 (6)	100

- 83% from gg processes
- additional partonic channels ($\mathrm{g}q$, $\mathrm{g}q$, $qq^{(\prime)}$) contribute 5%
- increase by only 8% relative to $\mathrm{pp} \to \mathrm{t\bar{t}b\bar{b}} \to \mathrm{l}^+\nu_\mathrm{l}\mathrm{jjb\bar{b}b\bar{b}}$ $(26.45 \to 28.60\,\mathrm{fb})$
- $\mathcal{O}\big((\alpha_\mathrm{s}^3\alpha)^2\big) < 2\%$
- interference pattern as for $\mathrm{pp} \to \mathrm{t\bar{t}b\bar{b}} \to \mathrm{l}^+\nu_\mathrm{l}\mathrm{jjb\bar{b}b\bar{b}}$

Irreducible background for distributions

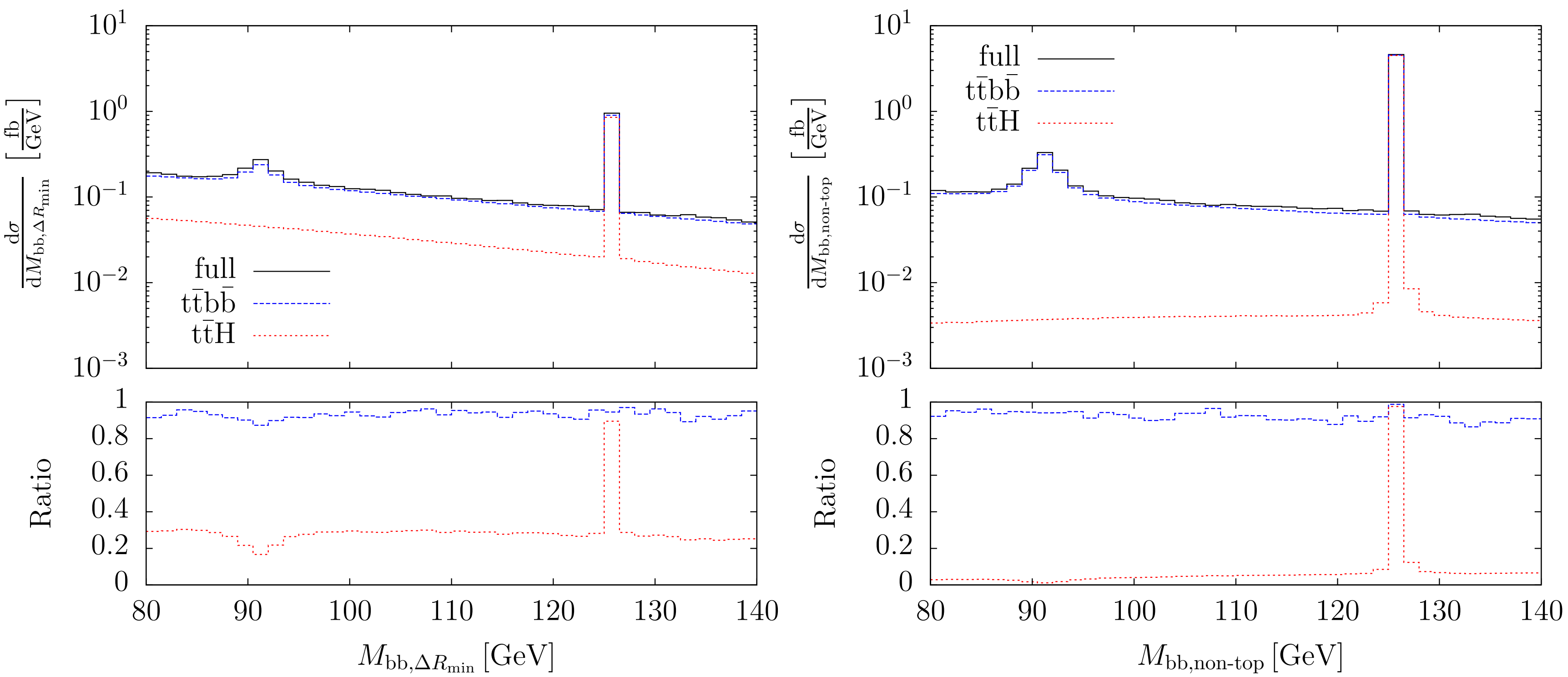

- invariant mass of b-jet pair with smallest ΔR distance:
  Higgs peak only weakly enhanced over combinatorial effect
  $\mathrm{t\bar{t}H/full} \sim 0.25$ (as for integrated cross section) outside resonances
- invariant mass of b-jet pair not resulting from top quarks:
  $\mathrm{t\bar{t}H/full}$ suppressed outside Higgs resonance (few per cent)
  Higgs resonance and Z resonance well tagged

Irreducible background for distributions

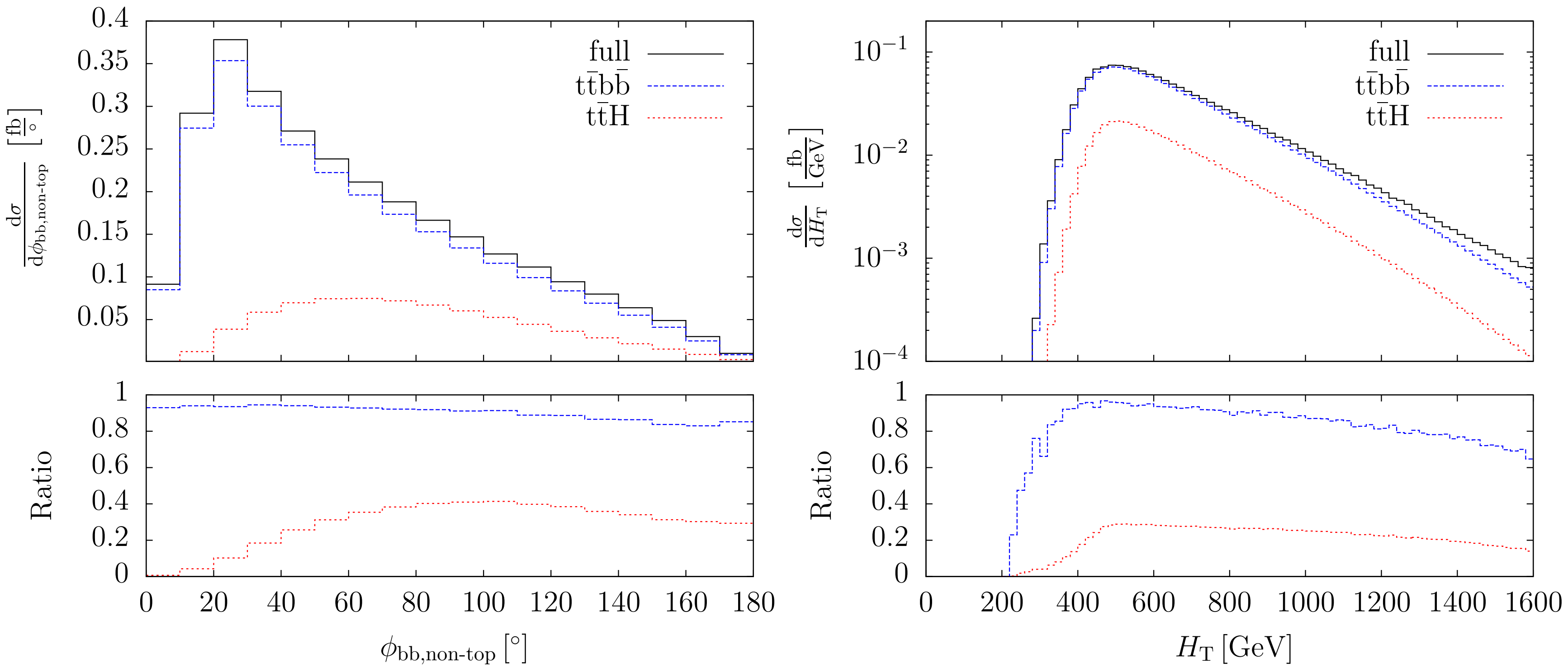

- azimuthal angle between b-jet pair not resulting from top quarks:
  background peaked at small angles ($\mathrm{b}\bar{\mathrm{b}}$ pair dominantly from gluons)
  signal prefers larger angles (massive Higgs boson)
- sum of all transverse energies H_T:
  signal suppressed for small H_T (ttH threshold)
  signal drops faster for large H_T (intermediate massive particles)
  behaviour typical for transverse-momentum distributions

Interference effects on distributions

Constant shift of -5% for most contributions with some exceptions

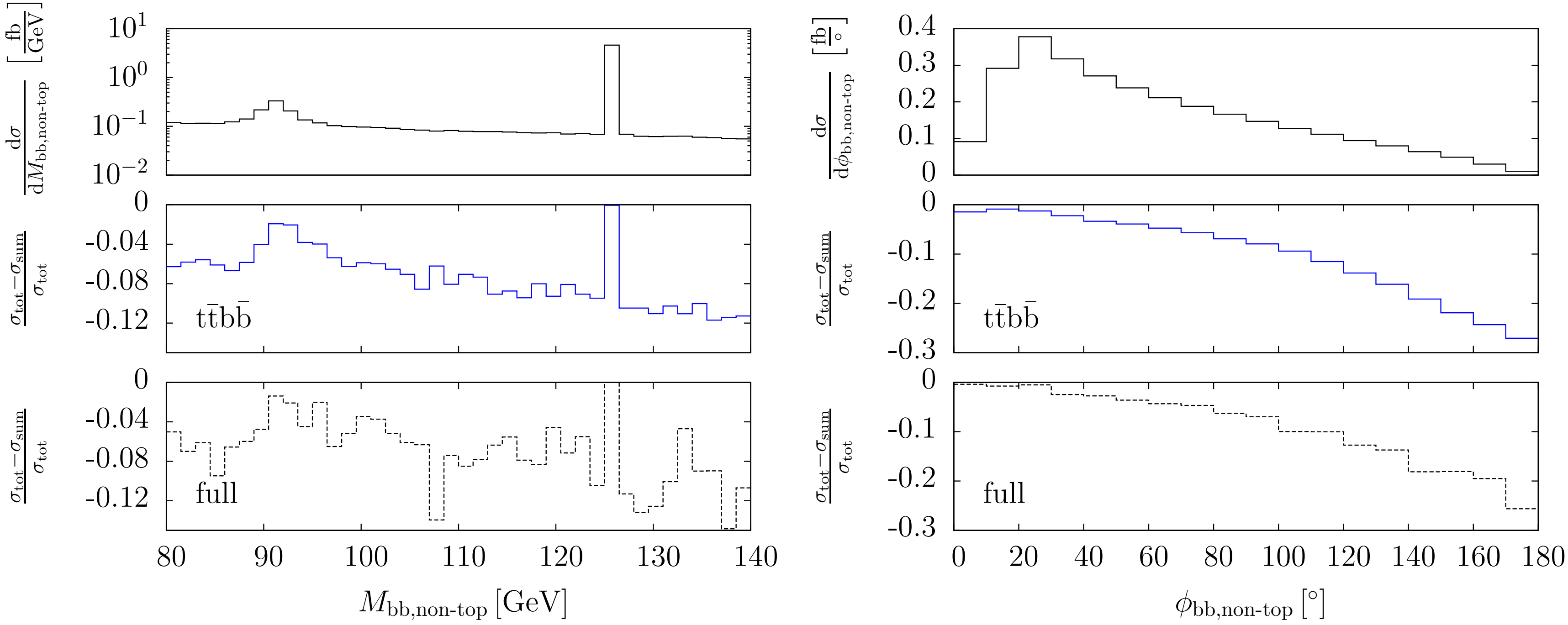

- invariant mass of $b\bar{b}$ pair not resulting from top quark:
  interference varies between 0% (on Higgs resonance) and -10%
- azimuthal angle between $b\bar{b}$ pair not resulting from top quark:
  large interference for large angles (suppressed cross section)

NLO QCD corrections to

$$\mathrm{pp} \to \mathrm{W^+W^-b\bar{b}H}$$

$\mathrm{pp} \to \mathrm{W^+W^-b\bar{b}H}$ at LO

Process: $\mathrm{pp} \to \mathrm{e^+}\nu_\mathrm{e}\mu^-\bar{\nu}_\mu\mathrm{b\bar{b}H}$
stable Higgs boson, but full top decays $\Rightarrow$

- misses substantial part of irreducible background to $\mathrm{t\bar{t}H}$ production
- includes all Higgs-production contributions
  also Higgs radiation from $\mathrm{W/Z}$ bosons (radiation from b quarks neglected)

partonic subprocesses

- $\mathrm{gg} \to \mathrm{e^+}\nu_\mathrm{e}\mu^-\bar{\nu}_\mu\mathrm{b\bar{b}H}$ $\quad\mathcal{O}(\alpha_\mathrm{s}\alpha^{5/2})$
- $q\bar{q} \to \mathrm{e^+}\nu_\mathrm{e}\mu^-\bar{\nu}_\mu\mathrm{b\bar{b}H}$ $\quad\mathcal{O}(\alpha_\mathrm{s}\alpha^{5/2})$

[$\mathcal{O}(\alpha^{7/2}) \sim 0.2\%$ of $\mathcal{O}(\alpha_\mathrm{s}\alpha^{5/2})$ at LO $\Rightarrow$ neglected]

sample diagrams

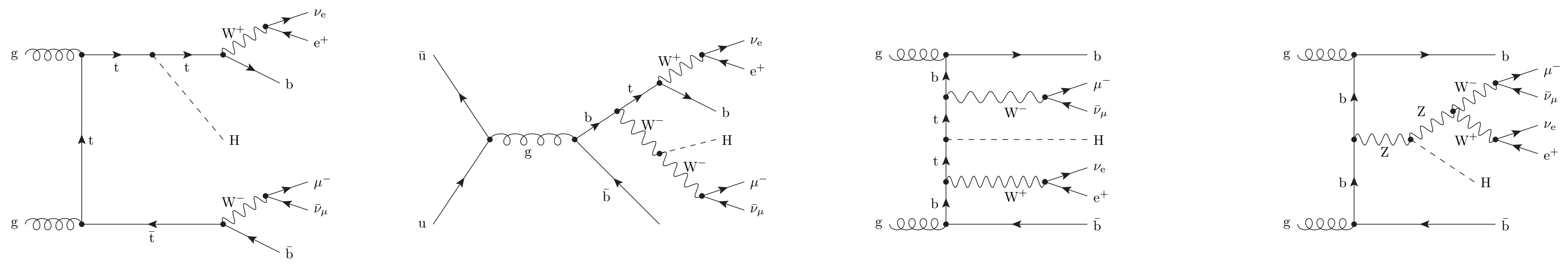

Existing NLO calculations

Results for signal process $\mathrm{pp} \to \mathrm{t\bar{t}H}$ (on-shell final-state particles)

- NLO QCD corrections ($\sim 20{-}30\%$) Beenakker et al. '01, 02', Dawson et al. '01–'03
  residual NLO scale uncertainty $\sim 10\%$
- NLO parton-shower matching Frederix et al. '11; Garzelli et al. '11
- NLO EW corrections Frixione et al. '14, '15 (stable top/Higgs); Zhang et al '14 (NWA)

results for dominant background process $\mathrm{pp} \to \mathrm{t\bar{t}b\bar{b}}$

- NLO QCD corrections Bredenstein et al. '08–'10; Bevilacqua et al. '09
- NLO parton-shower matching Kardos, Trócsányi '13
- NLO QCD corrections for massive bottom quarks and parton-shower matching Cascioli et al. '13

results for reducible background $\mathrm{t\bar{t}jj}$ (misidentified bottom quarks)

- NLO QCD corrections Bevilacqua et al. '10
- NLO parton-shower matching Höche et al. '14

$\mathrm{pp} \to \mathrm{W^+W^-b\bar{b}H}$ at NLO

Calculation follows in many respects the one for $\mathrm{pp} \to \mathrm{W^+W^-b\bar{b}}$

Denner, Dittmaier, Kallweit, Pozzorini ’11, ’12

- massless bottom quarks
- complex-mass scheme for t, Z, W — Denner, Dittmaier, Roth, Wieders ’99
- Catani–Seymour dipole subtraction for real corrections — Catani, Seymour ’97
  (same dipoles as for $\mathrm{pp} \to \mathrm{W^+W^-b\bar{b}}$) — Dittmaier ’99; Phaf, Weinzierl 01; Catani et al. ’02

differences

- all matrix elements calculated with RECOLA
- appearance of heptagons (7-point functions)

include only $\mathcal{O}(\alpha_s)$ corrections to $\mathcal{O}\left(\alpha_s\alpha^{5/2}\right)$ diagrams

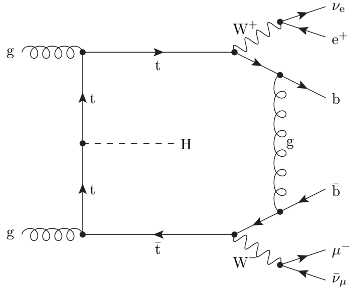

partonic processes for real corrections

- $\mathrm{gg} \to \mathrm{e^+}\nu_\mathrm{e}\mu^-\bar{\nu}_\mu\mathrm{b\bar{b}Hg}$
- $q\bar{q} \to \mathrm{e^+}\nu_\mathrm{e}\mu^-\bar{\nu}_\mu\mathrm{b\bar{b}Hg}$
- $\mathrm{g}\{q/\bar{q}\} \to \mathrm{e^+}\nu_\mathrm{e}\mu^-\bar{\nu}_\mu\mathrm{b\bar{b}H}\{q/\bar{q}\}$

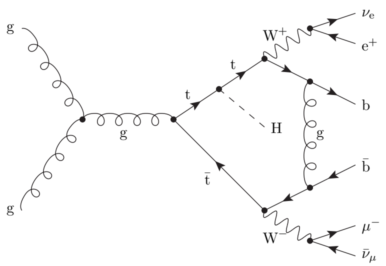

Implementation and checks

Setup for calculation

- (tree-level and one-loop) matrix elements with RECOLA
  (Recursive computation of one-loop amplitudes)
  Actis, Denner, Hofer, Scharf, Uccirati
- tensor integrals with COLLIER
  (Complex one-loop library in extended regularizations) Denner, Dittmaier, Hofer
- phase-space integration with in-house multi-channel Monte Carlo Feger

Checks

- LO and NLO matrix elements successfully compared with
  MADGRAPH5_AMC@NLO Alwall et al. '14
- Ward identities checked for $\mathrm{gg} \to \mathrm{W^+W^-b\bar{b}H}$ at LO and NLO
- process without Higgs compared in detail against original calculation of
  $\mathrm{pp} \to \mathrm{W^+W^-b\bar{b}}$ Denner, Dittmaier, Kallweit, Pozzorini '11, '12
  equivalent structure of real corrections and subtraction terms

Numerical accuracy of virtual corrections

Tuned comparison of virtual contributions between RECOLA and MADGRAPH5_AMC@NLO

Alwall et al. '14

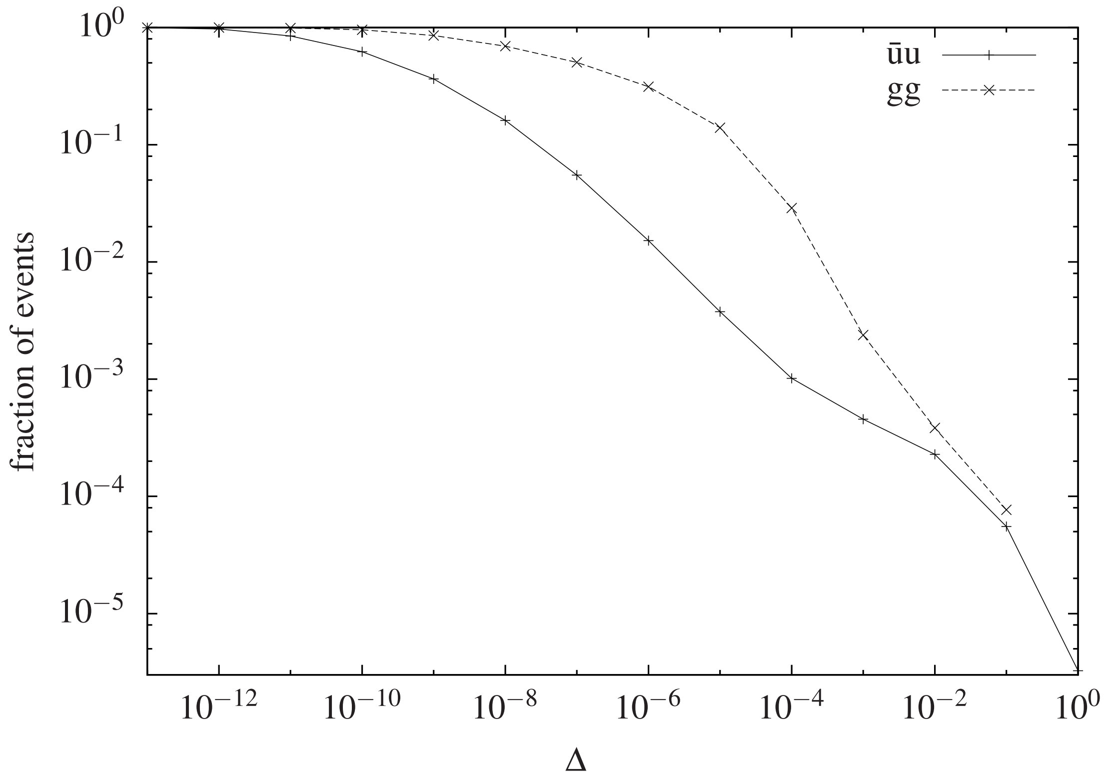

$$\Delta = \frac{(\mathrm{Re}\,\mathcal{M}_0^*\mathcal{M}_1)_{\mathrm{MG}}}{(\mathrm{Re}\,\mathcal{M}_0^*\mathcal{M}_1)_{\mathrm{Recola}}} - 1$$

- typical agreement:
  $10^{-5} - 10^{-10}$ for gg
  $10^{-8} - 10^{-12}$ for $\bar{\mathrm{u}}\mathrm{u}$
- agreement worse than 10^{-3} for less than 0.3% of points for gg
  0.04% of points for $\bar{\mathrm{u}}\mathrm{u}$

$\Rightarrow$

- convincing consistency check of MADGRAPH5_AMC@NLO and RECOLA
- successful check of 7-point functions in COLLIER
  yield substantial contribution to virtual corrections

Check of Ward identity

Numerical check of Ward identity for $\mathrm{gg} \to \mathrm{e}^+\nu_\mathrm{e}\mu^-\bar{\nu}_\mu\mathrm{H}$

(polarization vector of gluon replaced by normalized momentum p^μ/p_0)

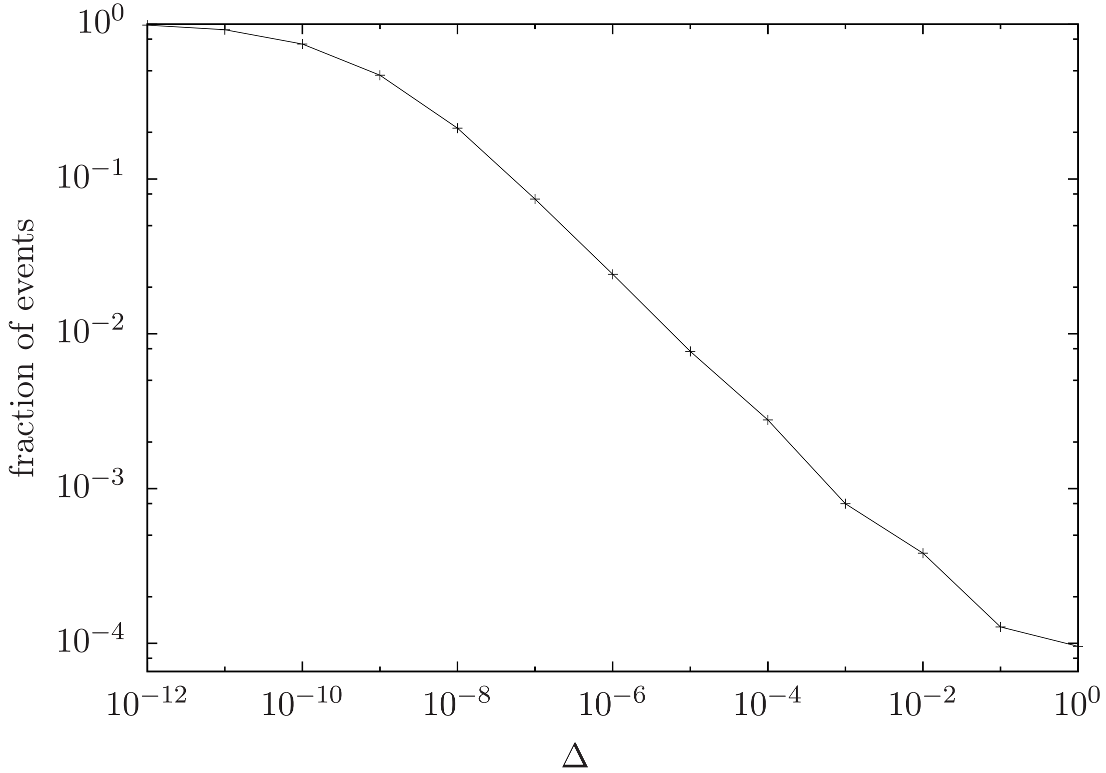

$$\Delta = \frac{\mathrm{Re}\,\mathcal{M}_1(\epsilon \to p/p_0)\mathcal{M}_0^*}{\mathrm{Re}\,\mathcal{M}_0^*\mathcal{M}_1}$$

- typical accuracy: $10^{-8} - 10^{-10}$
- agreement worse than 10^{-3} for less than 0.04% of points

$\Rightarrow$

- WI check comparable or better that comparison with MadLoop
- successful check of 7-point functions in Collier (yield substantial contribution to virtual corrections)

Comparison with literature

Total cross section for $\mathrm{pp} \to \mathrm{t\bar{t}H} \to \mathrm{e}^+\nu_\mathrm{e}\mu^-\bar{\nu}_\mu\mathrm{H}$ (without cuts)

Set-up:

- tuned parameters
- loose cuts: $p_{\mathrm{T,b}} > 2\,\mathrm{GeV}$, $\Delta R_{\mathrm{bb}} > 0.01$
  (needed for IR safety of irreducible background: $\mathrm{g} \to \mathrm{b\bar{b}}$ or $\mathrm{b} \parallel$ beam)
- $\mathcal{O}(\alpha_\mathrm{s}^2)$ matching correction according to Denner, Dittmaier, Kallweit, Pozzorini ’12
  (few per-cent effect)

agreement with literature at level of $1{-}2$ per cent

- with Beenakker et al. ’02:
  - agreement at LO: within 1.6%
  - agreement at NLO: within 0.1%
- with Frederix et al. ’11:
  - agreement at LO: within 1.6%
  - agreement at NLO: within 0.6%

Setup for phenomenological analysis

- pp collider energy: $13\,\mathrm{TeV}$
- PDFs: CT10 NLO Lai et al. '10
- scales:
  fixed scale: $\mu_\mathrm{R} = \mu_\mathrm{F} = m_\mathrm{t} + \frac{1}{2}M_\mathrm{H} = 236\,\mathrm{GeV}$ Beenakker et al. '03
  dynamical scale: $\mu_\mathrm{R} = \mu_\mathrm{F} = (m_{\mathrm{t,T}} m_{\bar{\mathrm{t}},\mathrm{T}} m_{\mathrm{H,T}})^{1/3}$ with $m_\mathrm{T} = \sqrt{m^2 + p_\mathrm{T}^2}$
  Frederix et al. '11
- LO/NLO top-quark width including off-shell W-boson effects ($\mathrm{t} \to \mathrm{bl}^+\nu_l$) from Jezabek, Kühn '89
- jet clustering: anti-k_T algorithm with $\Delta R = 0.4$ Cacciari, Salam, Soyez '08
- cuts: require two bottom jets and two charged leptons with

$$p_{\mathrm{T,b}} > 25\,\mathrm{GeV}, \quad |\eta_b| < 2.5$$
$$p_{\mathrm{T,l}} > 20\,\mathrm{GeV}, \quad |\eta_\mathrm{l}| < 2.5$$
$$p_{\mathrm{T,miss}} > 20\,\mathrm{GeV}$$
$$\Delta R_{\mathrm{bb}} > 0.4$$

Results for integrated cross section

μ_0	channel	σ_{LO} [fb]	σ_{NLO} [fb]	K
μ_{dyn}	gg	$1.5938(1)^{+33.8\%}_{-23.6\%}$	$2.026(3)^{-16.1\%}_{+0.9\%}$	1.271(2)
	$q\bar{q}$	$0.67520(5)^{+24.1\%}_{-18.1\%}$	$0.495(2)^{-39.5\%}_{+17.2\%}$	0.733(2)
	$\mathrm{g}\overset{(-)}{q}$		$0.1347(7)^{+298\%}_{-152\%}$	
	pp	$2.2690(1)^{+30.9\%}_{-22.0\%}$	$2.656(3)^{-4.6\%}_{-3.8\%}$	1.171(1)
μ_{fix}	gg	$1.5713(1)^{+34.0\%}_{-23.7\%}$	$2.010(3)^{-16.5\%}_{+1.0\%}$	1.279(2)
	$q\bar{q}$	$0.67235(5)^{+24.3\%}_{-18.2\%}$	$0.496(2)^{-39.3\%}_{+17.0\%}$	0.738(2)
	$\mathrm{g}\overset{(-)}{q}$		$0.1260(7)^{+312\%}_{-159\%}$	
	pp	$2.2436(1)^{+31.1\%}_{-22.1\%}$	$2.632(3)^{-5.1\%}_{-3.7\%}$	1.173(1)

- results for fixed and dynamical scale agree well
  logarithmic average: $\bar{\mu}_{\text{dyn}} = 222.3\,\text{GeV} \approx 236\,\text{GeV} = \mu_{\text{fix}}$
- K factor for $\mathrm{pp} \to \mathrm{t\bar{t}H}$ recovered
  [Beenakker et al. '03: $K \sim 1.2$, Frixione et al. '11: $K \sim 1.1$]
- reduction of scale dependence from 30% at LO to 5% at NLO

Scale dependence of integrated cross section

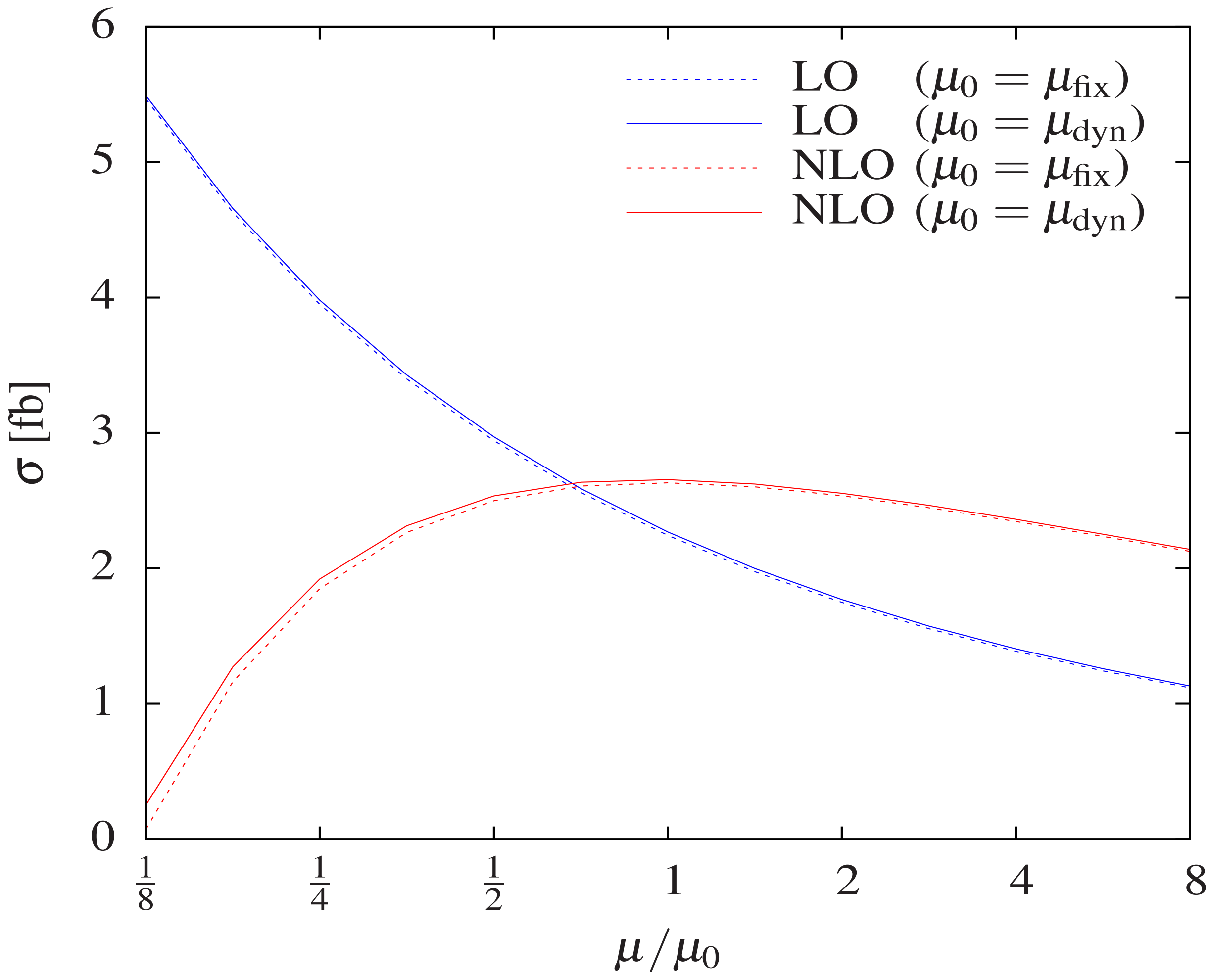

difference between fixed and dynamical scale 1%

Off-shell top effects on integrated cross section

Limit of on-shell top quarks

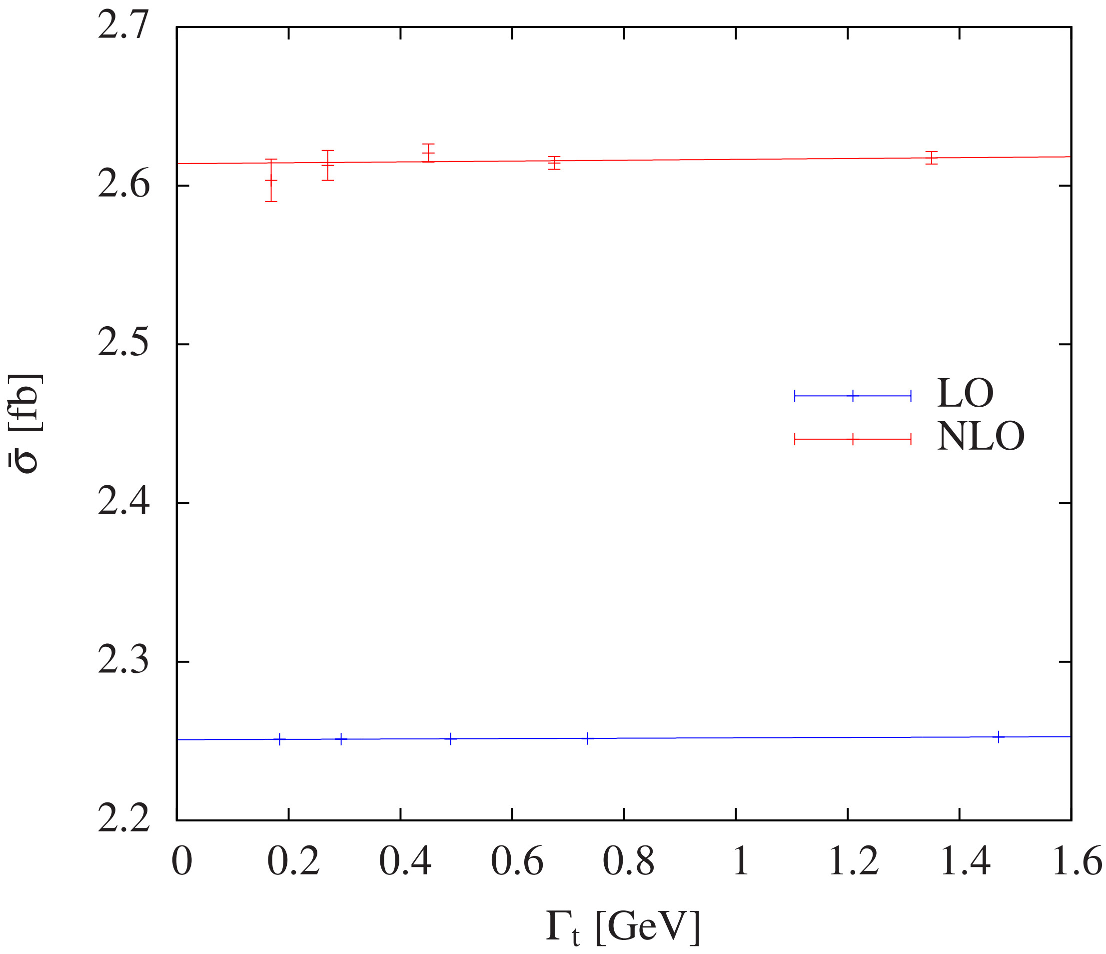

Extrapolate linearly

$\bar{\sigma}(\Gamma_t) = \sigma(\Gamma_t)\left(\frac{\Gamma_t}{\Gamma_t^{phys}}\right)^2$

to $\Gamma_t \to 0$

$\left(\frac{\Gamma_t}{\Gamma_t^{phys}}\right)^2$ corrects to physical branching ratios

$\bar{\sigma}(\Gamma_t \to 0)/\sigma(\Gamma_t^{phys}) - 1$

$= -0.08\%$ at LO

$= -0.14\%$ at NLO

(of order $\Gamma_t/m_t \sim 0.8\%$ as expected)

Transverse momentum distributions

fixed scale:

positron

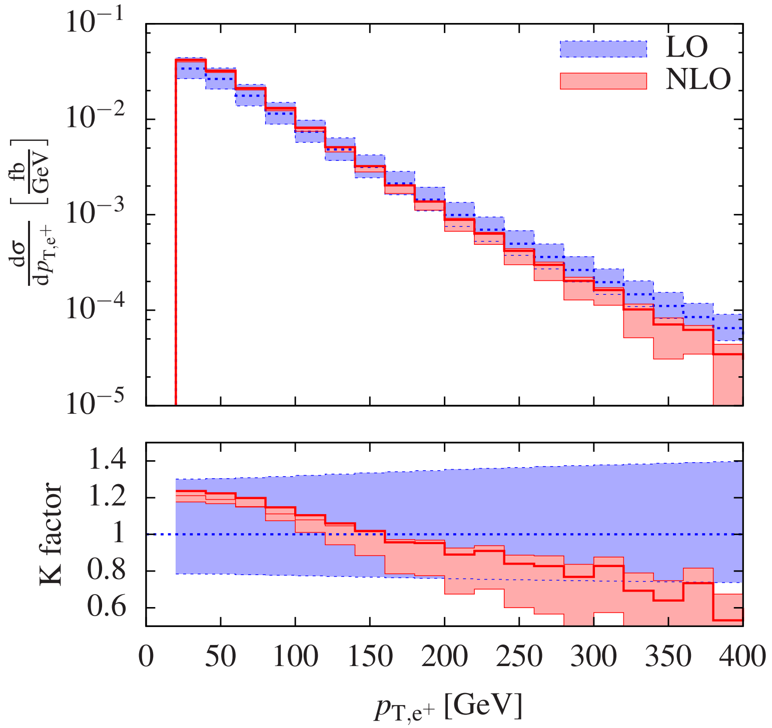

hardest bottom quark

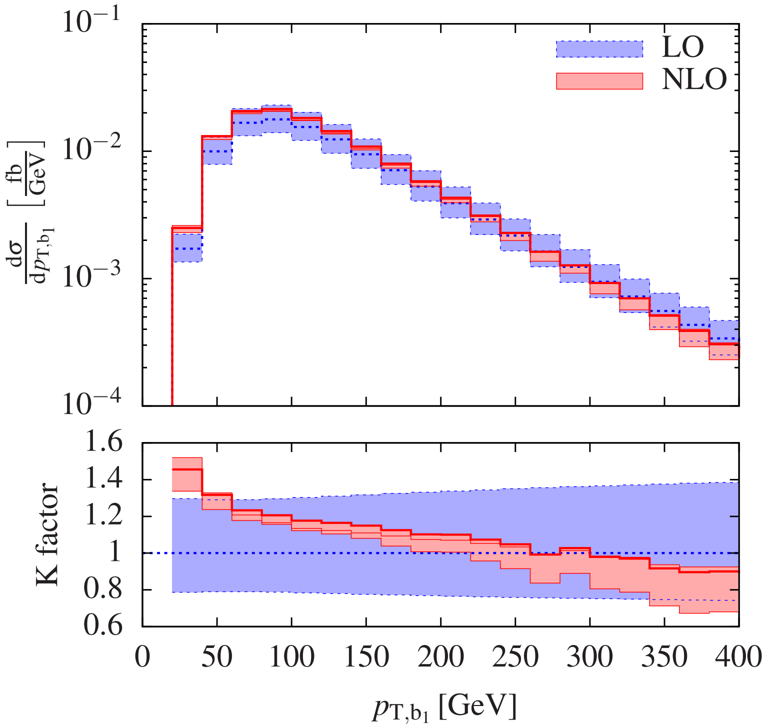

- steep drop of distributions
- K factor decreases strongly with p_T (almost factor 2 between 25 and $400\,\mathrm{GeV}$)

$$K_{LO} = d\sigma_{LO}(\mu)/d\sigma_{LO}(\mu_0)$$

$$K_{NLO} = d\sigma_{NLO}(\mu)/d\sigma_{LO}(\mu_0)$$

Transverse momentum distributions

dynamical scale:

positron | hardest bottom quark

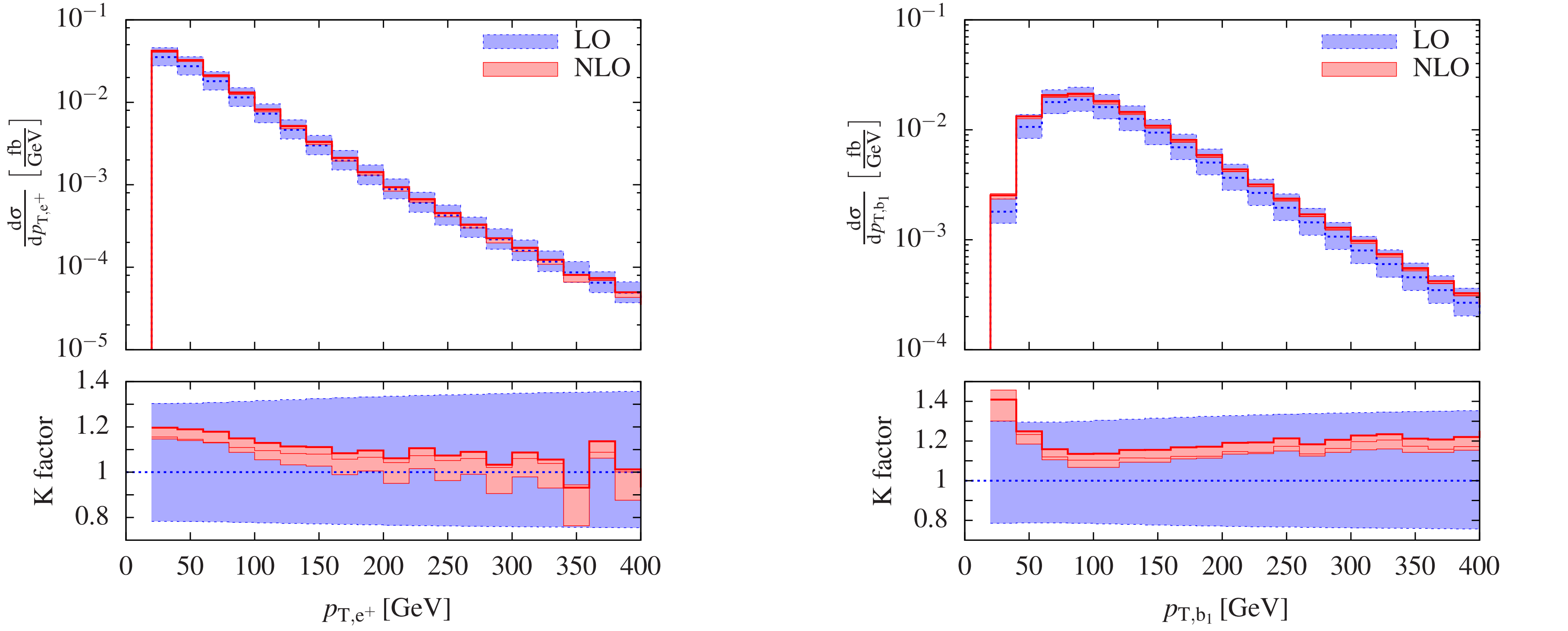

- K factor much flatter as function of p_T
  variation between 25 and $400\,\mathrm{GeV}$ within 20% and LO uncertainty band
- residual scale uncertainty $\sim 10\%$

Transverse momentum distributions

dynamical scale:

Higgs boson

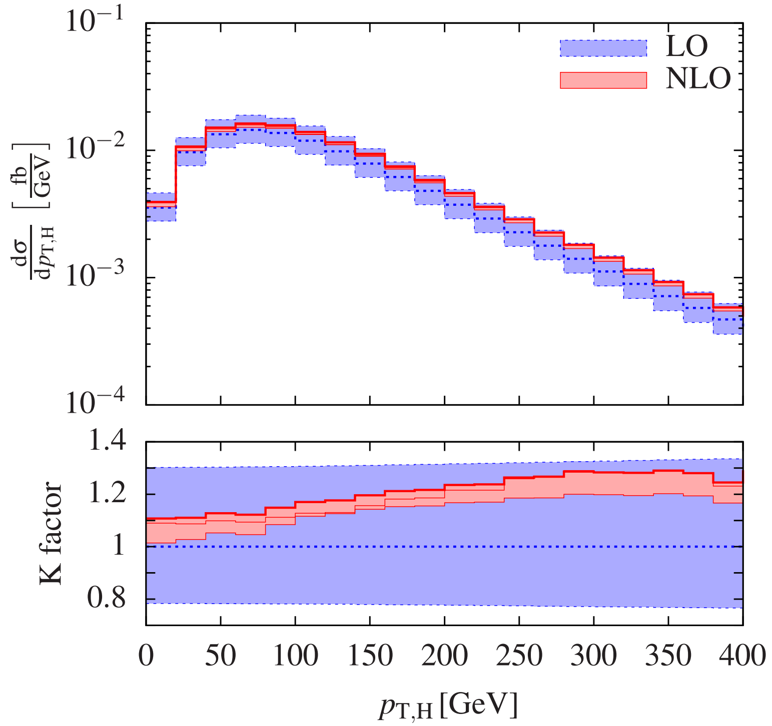

bottom quark pair

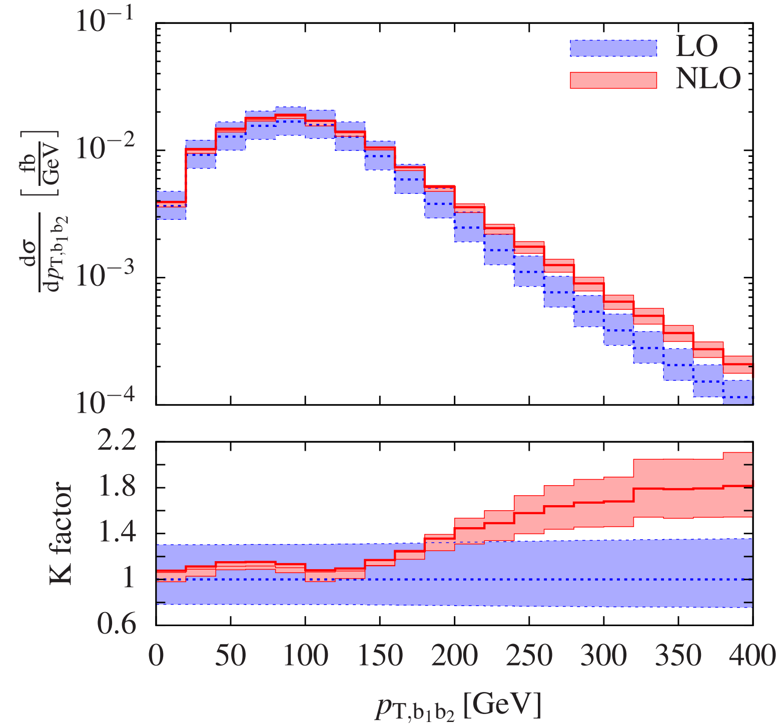

- K factor for Higgs-boson p_T within LO uncertainty band
- K factor for b-quark pair p_T increases for high transverse momentum
  (high $p_{T,bb}$ region suppressed for on-shell top quarks,
  even larger effect for $t\bar{t}$ production)

Angular/rapidity distributions

dynamical scale:

azimuth between leptons

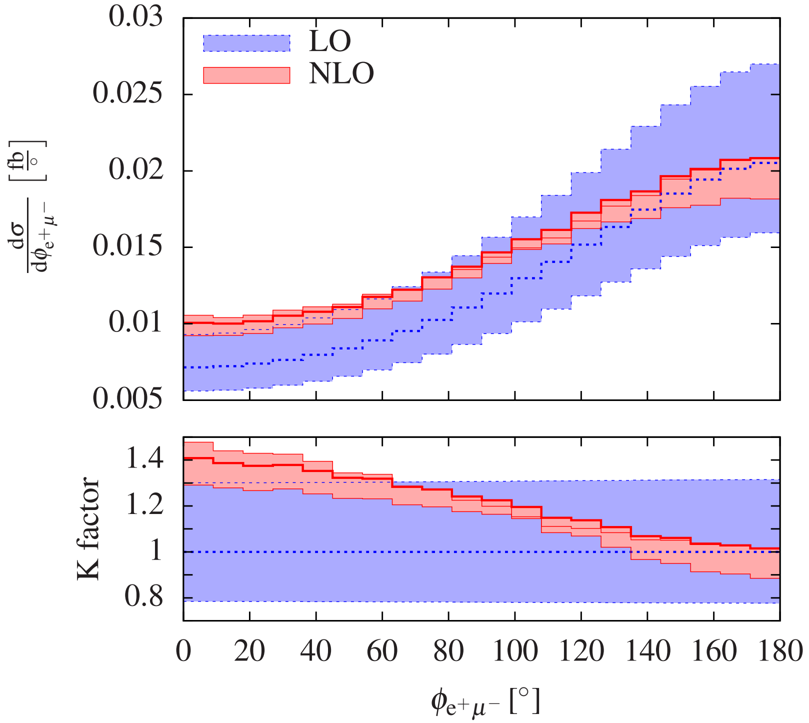

rapidity of Higgs boson

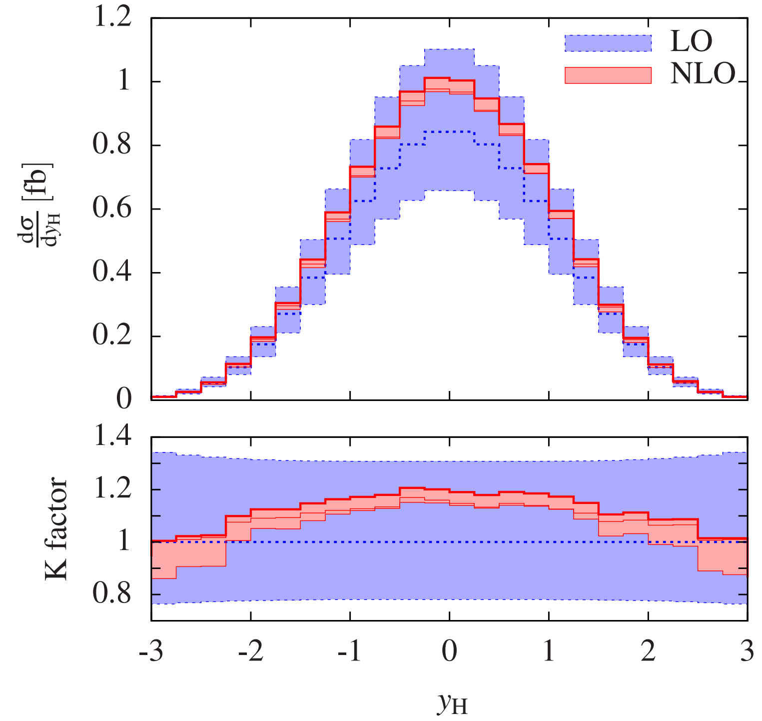

- NLO corrections shift events to small $\phi_{e^+\mu^-}$, 40% effect
  effect somewhat larger for fixed scale
- NLO corrections shift events to small Higgs-boson rapidity, 20% effect

Conclusions

Conclusions

Process $\mathrm{pp} \to \mathrm{t\bar{t}H}$ including top and Higgs decays investigated

- Leading-order analysis of $\mathrm{pp} \to \mathrm{l^+}\nu_\mathrm{l}\mathrm{jjb\bar{b}b\bar{b}}$
  - irreducible background $\sim 2.6\times$ signal at leading order
  - $\mathrm{pp} \to \mathrm{t\bar{t}b\bar{b}} \to \mathrm{l^+}\nu_\mathrm{l}\mathrm{jjb\bar{b}b\bar{b}}$ describes full process within 10%
  - sizeable interferences of -5% between QCD and EW diagrams flat for most but not all distributions
  - b-jet identification based on top-quark Breit–Wigners works well
- NLO QCD corrections to $\mathrm{pp} \to \mathrm{W^+W^-b\bar{b}H}$ $(\mathrm{pp} \to \mathrm{e^+}\nu_\mathrm{e}\mu^-\bar{\nu}_\mu\mathrm{b\bar{b}H})$
  - NLO corrections $\sim 17\%$ $(10{-}40\%$ for distributions)
  - scale dependence reduced to $5{-}10\%$
  - dynamical scale improves perturbative stability for large p_T
  - effects of top-quark decays on integrated cross section $< 1\%$
  - first calculation of $2 \to 5$ process with RECOLA and COLLIER
  - very good agreement of matrix elements with Madgraph5_aMC@NLO